HHS Public Access

Author manuscript

Eur J Cell Biol. Author manuscript; available in PMC 2018 March 01.

Published in final edited form as:

Eur J Cell Biol. 2017 March ; 96(2): 218–226. doi:10.1016/j.ejcb.2016.12.005.

EP4 RECEPTOR PROMOTES INVADOPODIA AND INVASION IN HUMAN BREAST CANCER

Felix Tönisen[1,2], **Louisiane Perrin**[2], **Battuya Bayarmagnai**[2], **Koen van den Dries**[1], **Alessandra Cambi**[1,*], and **Bojana Gligorijevic**[2,3,*]

[1]Department of Cell Biology, Radboud Institute for Molecular Life Science, Radboud University Medical Center, Geert Grooteplein 28, 6525 GA Nijmegen, The Netherlands [2]Department of Bioengineering, Temple University, 1947 N 12th St, 19122 Philadelphia, PA, USA [3]Fox Chase Cancer Center, Cancer Biology Program, Philadelphia, Pennsylvania, USA

Abstract

The production of Prostaglandin E_2 (PGE_2) is elevated in human breast cancer cells. The abnormal expression of COX-2, which is involved in the synthesis of PGE_2, was recently reported as a critical determinant for invasiveness of human breast cancer cells. Autocrine and paracrine PGE_2-mediated stimulation of the PGE_2 receptor EP4 transduces multiple signaling pathways leading to diverse patho-physiological effects, including tumor cell invasion and metastasis. It is known that PGE_2-induced EP4 activation can transactivate the intracellular signaling pathway of the epidermal growth factor receptor (EGFR). In malignant cancer cells, EGFR pathway activation promotes invadopodia protrusions, which further leads to degradation of the surrounding extracellular matrix (ECM). Despite the known influence of EP4 on the EGFR signaling pathway, the effect of EP4 stimulation on invadopodia formation in human breast cancer was never tested directly. Here we demonstrate the involvement of EP4 in invasion and its effect on invadopodia in breast cancer MDA-MB-231 cells using 2D invadopodia and 3D invasion *in vitro* assays as well as intravital microscopy. The results show that stimulation with the selective EP4 agonist CAY10598 or PGE_2 promotes invadopodia-mediated degradation of the ECM, as well as the invasion of breast cancer cells in *in vitro* models. The effect on matrix degradation can be abrogated via direct inhibition of EP4 signaling as well as via inhibition of EGFR tyrosine kinase, indicating that EP4-mediated effects on invadopodia-driven degradation are EGFR dependent. Finally, using xenograft mouse models, we show that short-term systemic treatment with CAY10598 results in a >9-fold increase in the number of invadopodia. These findings highlight the importance of further investigation on the role of EP4-EGFR crosstalk in invadopodia formation.

Correspondence to bojana.gligorijevic@temple.edu.

*Authors equally contributed to this manuscript

Authors contributions

FT, BG and AC conceived and designed the experiments. BB and FT performed the 3D invasion experiments; LP and FT performed the invadopodia experiments; FT performed the intravital microscopy experiments. FT, LP and BB collected and analyzed the data. FT, LP, LL, KD, BG and AC interpreted the data. FT, BG and AC wrote the manuscript.

Keywords

invadopodia; invasion; prostaglandin E_2; EP4; spheroids; intravital microscopy

INTRODUCTION

During tumor progression, cancer cells develop the ability to degrade the extracellular matrix that allows them to move through the surrounding tissue and to breach blood vessel walls (Martin et al., 2000). This results in intravasation, the process of cancer cells entry into the blood vessels. Cancer cells further spread to secondary organs, where they can form metastases that are the main cause of patient mortality in most solid cancers.

Invadopodia, protrusions rich in F-actin and capable of degrading a number of proteins in extracellular matrix (ECM), have been hypothesized to facilitate the breach of the basement membrane necessary for several steps in metastasis (Beaty and Condeelis, 2014). Recent studies revealed that invadopodia assembly is directly molecularly linked with metastasis in mouse models and humans (Eckert et al., 2011; Gligorijevic et al., 2012). Further, real-time imaging in mice provided evidence that invadopodia are essential for both intravasation and extravasation of cancer cells into/from the blood vessels (Gligorijevic et al., 2014; Leong et al., 2014).

The assembly and maturation of invadopodia can be initiated by chemical stimuli such as the epidermal growth factor (EGF), as well as the mechanical signals from extracellular matrix (ECM). Upon binding, EGF activates the EGF receptor (EGFR), which further activates several intracellular signaling pathways (Cortesio et al., 2008), including the Src kinase which mediates the assembly of the invadopodium precursor and the phosphoinositide-3 kinase (PI-3K), necessary for anchoring the precursor to the cell membrane (Beaty and Condeelis, 2014). In addition to EGF, several other growth factors have been shown to initiate invadopodia formation. For example, transforming growth factor-β (TGF-β), platelet-derived growth factor (PDGF), hepatocyte growth factor (HGF) and heparin binding EGF (HB-EGF) can induce invadopodia formation in several types of cancer cells (Díaz et al., 2013; Eckert et al., 2011; Pignatelli et al., 2012; Rajadurai et al., 2012; Yamaguchi et al., 2005). Moreover, autocrine signals can lead to the induction of invadopodium formation (Patsialou et al., 2009).

In addition to growth factors, a number of signals present in the tumor microenvironment, such as hypoxia, pH or direct interactions with stromal cells were shown to be associated with invasion and metastasis of cancer cells (Gould and Courtneidge, 2014). The production of the pro-inflammatory lipid Prostaglandin E_2 (PGE_2) is elevated in breast cancer due to high expression of the prostaglandin-endoperoxidase synthase 2 (COX2), which is a critical determinant for invasiveness of human breast cancer cells (Bocca et al., 2014; Miglietta et al., 2010; Park et al., 2012). However, the direct link between elevated PGE_2 and increased invasiveness of human breast cancer cells remains elusive. PGE_2 activity is mediated by four G-protein coupled receptor isotypes called EP1, -2, -3 and -4 (Narumiya et al., 1999; Pierce and Regan, 1998). The activation of the PGE_2 receptor EP4 subtype (EP4) by its ligand PGE_2 is known as a mechanism that increases the invasive capability of cancer cells (Konya

et al., 2013). Hence, it is likely that EP4 is involved in the PGE_2-mediated increase of cancer invasiveness. EP4 is capable of activating distinct intracellular signaling pathways. Its signaling is associated with the stimulating G alpha protein ($G\alpha_s$), which leads to an increase of the intracellular secondary messenger cyclic adenosine monophosphate (cAMP) (Regan, 2003). Furthermore, EP4 is also capable of inhibiting the formation of cAMP by activating the inhibiting G alpha protein ($G\alpha_i$) (Fujino and Regan, 2006).

The activated EP4 can be phosphorylated by a G protein-coupled receptor kinase (GRK), which enables the recruitment of β-arrestin to EP4 (Konya et al., 2013; Yokoyama et al., 2013). The EP4/β-arrestin complex then activates the membrane-bound Src, which is able to transactivate the EGFR receptor, thus showing that the EP4/β-arrestin/Src complex facilitates cell migration and metastasis (Buchanan et al., 2006; Kim et al., 2010). Moreover, it has been demonstrated that Src, activated by the EP4 signaling pathway, can also activate PI-3K (Yokoyama et al., 2013). This signaling cascade was demonstrated previously to be active in the migration and metastasis processes in colorectal carcinomas (Buchanan et al., 2006; Konya et al., 2013).

Taken collectively, these data demonstrate that stimulation of EP4 increases invasive behavior of cancer cells and that the EP4 and EGFR pathways cross-talk. However, the direct relationship between EP4 stimulation by PGE_2 and invadopodia formation has not been studied yet. Here we focus on testing if EP4 stimulation influences invadopodia assembly and ECM degradation. Using *in vitro* invadopodia and spheroid assays as well as intravital imaging, our results provide novel insights into the effects of EP4 activation on breast cancer invasion. Understanding the interplay between different signaling receptors promoting cancer cell invasive behavior may provide novel targets to prevent or reduce cancer dissemination and metastasis.

RESULTS

Biphasic dose response of EGFR or EP4 on invasion of MDA-MB-231 cells

Cell cultures in 3D, including spheroids and related assays, have been exhaustively shown to better mimic physiological effects on cultured cells compared to 2D assays (Boudreau et al., 1996; Cukierman et al., 2002). Moreover, since the demonstration that MMP activity is necessary for the invasion of spheroids into the acid-soluble rat-tail collagen I (Sodek et al., 2008), spheroids are replacing the previous transwell assay, becoming a new standard for studying the invasiveness of cells (Friedl et al., 2012). Figure 1A shows representative spheroids of control (starved cells with no stimulation) as well as MDA-MB-231 cells stimulated by EGF-, CAY10598- (EP4 agonist) and PGE_2. Dose-response curves of EGF, CAY10598 and PGE_2 were obtained after 24 (light bars) and 48 h (dark bars, Figure 1B–D). To compare differences in the extent of cell invasion, the relative invasion area was calculated (see Materials and Methods; **Figure S1**). Figure 1B shows 1 nM is the peak of the biphasic response to EGF- stimulated invasion. EP4 agonist CAY10598 and PGE_2 treatments showed peaks in their responses at a dose of 10 nM and 100 nM, respectively (Figure 1C, D). Following dose response determination, we proceeded with optimal doses determined, optimizing and automating the spheroid assay towards more precise high-throughput results.

EGFR and EP4 stimulation significantly increase the invasive capability of MDA-MB-231 cells

We next stained spheroids after 48 h with DAPI. This allowed a more accurate examination of invasion by quantification of nuclei in the invasion zone. Figure 2A shows representative images of control condition (starved cells with addition of DMSO), as well as EGF-, CAY10598- and PGE_2-stimulated conditions. In Figure 2B, the automated analysis pipeline is demonstrated. First, the core is subtracted from the image followed by nuclei segmentation and quantification (see Materials and Methods). Under stimulation with EGF, a higher number of cells invade into the ECM and the invasion distance is higher compared to the control condition (Figure 2A, C). Similarly, the number of invading MDA-MB-231 cells was also significantly elevated by stimulation with CAY10598 or PGE_2, suggesting that stimulation of EP4 induces invasion in 3D (Figure 2A, C). In the presence of the cell proliferation-inhibiting agent Mitomycin C, EGF stimulation still increases the number of cells in the invasion zone (Figure 2D) (An et al., 2015). This clearly indicates that the observed effect is due to invasion and not proliferation.

EGFR and EP4 affect invadopodia maturation and degradative capability

To investigate the role of EP4 in invadopodia stimulation, MDA-MB-231 cells plated on fluorescent gelatin were fixed after 16 hours (Figure 3A, left two panels) and the number of cells with mature invadopodia as well as the cumulative area of gelatin degradation were measured. Degradative activity of invadopodia was detected as non-fluorescent (dark) punctae inside fluorescent gelatin (Figure 3A, left). Mature invadopodia are represented as punctae with co-localized gelatin degradation and cortactin staining (Figure 3A, panels on the right). The measurements of the degradation area indicated that EGF, CAY10598 and PGE_2 increase matrix degradation (Figure 3B). Similar measurements of invadopodia precursors did not show significant increase upon stimulation (data not shown). As expected, inhibition of the EGFR tyrosine kinase with gefitinib (Iressa) reversed the effect of EGF on degradation capability. Interestingly, the effect of CAY10598 and PGE_2 on the degradation capability was also inhibited by gefitinib. This indicates that the EGFR tyrosine kinase is crucial for EP4-mediated stimulation of invadopodia. Inhibition of EP4 with GW627368X, a selective competitive antagonist, reverses the effect of PGE_2 as well as EGF on degradation, indicating a crosstalk between EGFR and EP4. In contrast, GW627368X did not block CAY10598-induced stimulation significantly. This might be due to higher on/off ratio of EP4 and CAY10598 compared to EP4 and GW627368X, caused by differential binding affinities for EP4. In line with the gelatin degradation results, the number of cells with mature invadopodia was also significantly affected (Figure 3C). Again, GW627368X or gefitinib were used in order to test if the effect on invadopodia by the stimulants can be inhibited. Only inhibition of the EGFR was able to reverse the effect of EGF or CAY10598 significantly. To more directly test EP4 and PGE_2 involvement in the invadopodia, we have further used siRNA-mediated knock-down of EP4. Both the degradative effect and the effect on the number of cells with mature invadopodia by PGE_2 stimulation were abrogated by EP4 knock-down (Figure 3D, E). The knock-down of EP4 was confirmed by immunofluorescent staining and Western Blot of siCtrl- or siEP4-transfected MDA-MB-231 cells (Figure 3F, G). While the knock-down levels (51% for siEP4 #1 and 52% for siEP4 #2)

seem to directly correlate to the number of mature invadopodia, both siEP4 knock-downs showed almost complete abrogation of the 16h-cumulative degradation.

To assess the effect of EP4 stimulation on degradative capability in 3D spheroid assay, MDA-MB-231 spheroids were fixed and labeled at 48h. They were further stained for cortactin, F-actin and collagen I (3/4) antibody that binds to degraded collagen fibrils and demonstrated the trace of the invading cancer cell (Figure 3H) (Gligorijevic et al., 2012; Wolf et al., 2007). Similar cell paths were previously reported as single cell invasion tunnels and found to enable MMP-independent migration of following cancer cells (Fisher et al., 2009). Collagen I 3/4 staining of control and CAY10598-treated spheroids were compared (Figure 3I, J), indicating that stimulation with CAY10598 increases the degradative capability in 3D. Taken together, these results clearly suggest an association between stimulation of EP4 and an increased matrix degradation as well as an elevated level of invadopodia-driven ECM degradation.

Intravital Microscopy suggests role of EP4 in invadopodia stimulation in breast cancer cells

Multiphoton intravital imaging of Dendra2-MDA-MB-231 xenografts (Figure 4A) confirmed the results of *in vitro* assays (Figure 3). Time-lapse imaging of the xenografts was done exclusively in perivascular regions containing major blood vessels and high density of collagen fibers, where invadopodia can be detected by morphodynamic analysis (Figure 4A; Video S1). EP4 stimulation led to the 9-fold increase in the formation of invadopodia (Figure 4B) in perivascular niches (Gligorijevic et al., 2014), following a systemic delivery via intraperitoneal injection 4h earlier. The stills from invadopodia time-lapse show extension of invadopodia *in vivo* (Figure 4C; Video S2).

DISCUSSION

In this study, we investigated the role of EP4 on invasion and invadopodia in breast cancer cells. Our results demonstrate that EP4 activation promotes invadopodia-driven ECM degradation, in turn facilitating future intravasation and metastasis of breast cancer cells (Gligorijevic et al., 2012; Gligorijevic et al., 2014).

Our data demonstrates that EP4 stimulation elevates the invasive capability of breast cancer cells in ways similar to EGFR stimulation. Interestingly, both EGF and CAY10598-induced stimulation of EGFR and EP4 exhibit biphasic dose responses. It was recently suggested that two phosphorylation sites at Src are involved in this dose-dependent switch in EGF signaling, Src-Y416, which activates Src at low EGF concentrations, and the Src-527, which inactivates it at high EGF concentrations (X. Zhang et al., 2012). The fact that CAY10598 also exhibits the biphasic response may suggest that EP4 mediates the effect on the invasive capability via Src. The presence of EP4 and EGFR signaling cross-talk is supported by the fact that inhibition of EGFR reverses the positive effect of EP4 stimulation on matrix degradation, and the other way around. A number of papers proposed the EGFR pathway as effector for EP4-mediated signaling pathways in cancer (Du et al., 2015; Parida et al., 2016; Tveteraas et al., 2012; Yokoyama et al., 2013; M. Zhang et al., 2014). Recently, it has been

shown that the selective EP4 inhibitor GW627368X restricts EGFR transactivation (Parida et al., 2016).

We here demonstrate that EP4 is capable of activating invadopodia-driven ECM degradation *in vitro* and might also be involved in ECM remodeling *in vivo*. This activation is dependent on the transactivation of the EGFR. The proposed signaling pathway, based on our findings and on existing literature (Buchanan et al., 2006; Kedziora et al., 2016), mediating the effect of EP4 on invadopodia maturation is depicted in Figure 5. Furthermore, we have shown that PGE_2, or specific EP4 stimulation with CAY10598, can promote invadopodia in the absence of EGF. A substitutive effect of PGE_2 on the EGFR signaling has been reported by Brocard et al., 2015 (Brocard et al., 2015).

It is important to note that MDA-MB-231 cells are reported to express also EP1 and EP3 (Paquette et al., 2011). The activation of all present EP receptors might result in a complex interplay and intracellular processing of the signals. The dissection of the contribution of each receptor in transducing PGE_2-dependent invasion and invadopodia signaling is a complex endeavor, but necessary to better understand the role of EP4 in particular. However, our preliminary results with EP2 specific agonist Butaprost showed it does not induce invasion and therefore EP2 is most likely not involved in promoting invasion (data not shown). Moreover, there was no significant difference in the stimulation of invadopodia matrix degradation as well as mature invadopodia between cells stimulated with the EP4-specific agonist CAY10598 and PGE_2, which can activate all four EP receptors subtypes. This indicates that PGE_2 mainly affects degradation and invadopodia through activation of EP4.

In summary, we have shown that EP4 stimulation increases the invasive capability of breast cancer cells as well as the degradative capability of invadopodia. Recently invadopodia became a very interesting therapeutic target for aggressive cancer because their inhibition is effective to limit invasion, extravasation and subsequent metastasis (Stoletov and Lewis, 2015). Since EP4 has been proposed as potential anti-cancer treatments (Kundu et al., 2014; Majumder et al., 2014) (Kundu et al., 2014; Majumder et al., 2014), further investigation of EP4 targeting to restrict invadopodia formation and cancer cell invasion is warranted.

MATERIALS AND METHODS

Cell culture and Animal Model

MDA-MB-231 cells (for high spheroid invasion assay, Invadopodium degradation assay) and Dendra2-MDA-MB-231 (for xenograft injection) were cultured in DMEM supplemented with 10% FBS, 50 units/mL penicillin and 50 μg/mL streptomycin. For serum starvation, cells at 70 % confluence were rinsed with PBS and starved in 0.5% FBS for 16–24 h.

Tumor formation in mice was carried out as described previously (Gligorijevic et al., 2014). Briefly, 10^6 Dendra2-MDA-MB-231 cells in 150 μl of 20% collagen I in PBS were injected into the mammary fat pads of 5–7 week old SCID mice. Intravital microscopy was done 12–18 weeks after injection, when tumors reached the size of 0.8–1 cm.

Spheroid Invasion Assay

The spheroids were formed by the hanging drop method with 1,000 cells/spheroid in DMEM containing 5.8% FBS, 50 units/mL penicillin and 50 μg/mL streptomycin, 4.8 mg/ml methyl cellulose and 20 μg/ml Nutragen (Advanced BioMatrix Inc., San Diego, CA) for 48 h. Then, the spheroids were embedded in 50 μl of 5 mg/ml rat-tail collagen I (Corning Inc., Corning, NY) and dispensed into each well of a 24-well plate. The collagen solution was prepared according to the manufacturer's protocol (Alternate Gelation Procedure). Next, 500 μl of DMEM containing 0.5% FBS, 50 units/mL penicillin, 50 μg/mL streptomycin and the test substances were added into each well. The embedded spheroids were incubated for 48 h, fixed with 4% PFA and stained with DAPI. The images were captured using the Olympus laser-scanning confocal microscope (Fluoview 1200 IX 83).

For the image analysis of unstained spheroids (Figure 1), both the core and the distal margin of the invasion zone were outlined manually based on phase-contrast images. Then, the area of the core was subtracted to obtain the area of the invasion zone.

For the image analysis of DAPI-stained spheroids (Figure 2), a custom macro was used in Fiji. Briefly, the images were preprocessed by applying a Gaussian blur filter to reduce noise. Next, the core of the spheroid was selected using inverted threshold and subtracted from each slice semi-automatically. Further, we used a local adaptive threshold algorithm from Fiji (Auto Local Threshold, Bernsen method) for thresholding. Then a Median filter was applied to the thresholded image and the Watershed function was used to allow segmentation of nearby nuclei. The Particle Analyzer was then used for the segmentation and quantification of nuclei.

EP4 siRNA transfection

MDA-MB-231 cells were transfected using the Amaxa® Cell Line Nucleofector® Kit V, according to the manufacturer's protocol. Briefly, 10^6 cells were resuspended in 100 μl Nucleofector® Solution and combined with 50 nM siRNA EP4 (Dharmacon, J-005714-06, siEP4 #1 and J-005714-07, siEP4 #2) or non-targeting control siRNA (Dharmacon, D-001810-01-05, siCtl). Samples were transferred into a 6-well plate and after 24 h, cells were serum-starved for 20 h before performing the invadopodium matrix degradation assay. Assessment of the knock-down efficiency was performed after 24 h by western-blot and immunofluorescence with EP4 antibody (Santa Cruz sc-55596; 1:100).

Invadopodium Matrix Degradation Assay

Lyophilized gelatin from pig skin, Oregon Green 488 conjugate (Life Technologies, Carlsbad, CA) was reconstituted in 2.5 ml H_20 containing 2 mM NaN_3 and stored at −20° C. For the preparation of a 0.2 % unlabeled gelatin solution, 50 mg gelatin from pig skin was dissolved in 25 mL PBS. The protocol for the preparation of fluorescent gelatin-coated dishes was adapted from Sharma et al. 2013 (Sharma et al., 2013). Briefly, MatTek dishes (MatTek corp., Ashland, MA) were treated with 300 μl 1N HCl for 10 min at room temperature. Between each of the subsequent steps the dishes were washed three times with PBS in 5 min intervals. Next, dishes were coated with 300 μl 50 μg/ml poly-L-lysine solution for 20 min at room temperature. Oregon Green 488 dye-labeled gelatin and

unlabeled gelatin were brought to room temperature before mixing them to make solutions with a final ratio of 1:20. The mixture was incubated for 5–10 min at 37° C prior 200 μl of this solution was added to the dish for 10 min at room temperature. Dishes were then transferred on ice and gelatin was cross-linked with 2 mL of chilled 0.2% glutaraldehyde solution on ice for 15 min and then quenched with 2 mL of fresh 5 mg/ml sodium borohydride solution for 15 min at room temperature. For sterilization, 2 mL 70% ethanol was added and incubated for 15 min at room temperature. After addition of 2 mL 1,000 units/mL penicillin and 1,000 μg/mL streptomycin in PBS, the dishes were stored at 4° C for up to 10 days before using them.

Serum-starved cells (20,000) were plated on the gelatin-coated dishes at 0 hours in culturing media with addition of 1 μM DMSO, 1 nM EGF, 10 nM CAY10598 (CAY) or 1 μM PGE_2. Treatments with inhibitors were done by adding 1μM GW627368X or 1 μM gefitinib to 1 nM EGF, 10 nM CAY10598 (CAY) or 1 μM PGE_2, respectively. At 16 hours, dishes were fixed and staining with anti-cortactin antibody was used for the identification and quantification of invadopodia. The stacks were processed and analyzed in a custom plugin for ImageJ. Briefly, images of a stack were combined using average intensity projection. For the analysis of degradation, Subtract Background plugin was used to correct for unevenness of the coating, images were thresholded and degradation holes were measured with Particle Analyzer. Invadopodia, defined as punctae co-localizing in cortactin and gelatin degradation were counted manually with the Multi-point tool.

Immunofluorescence

Cells were fixed with 4% paraformaldehyde in PBS for 15 min, permeabilized with 0.1% Triton-X100 in PBS for 5 min and blocked with 1% FBS/1% BSA in PBS for 2 h. Next, cells were incubated with the primary antibody in blocking buffer for 60–90 min, followed by the secondary antibody (1:250) in blocking buffer for 30 min. Primary antibodies against cortactin (Abcam ab33333; 1:100), EP4 (Santa Cruz sc-55596; 1:100) and degraded collagen I (Col I (3/4), ImmunoGlobe GmbH, Germany, 1:100) were used. For staining of spheroids embedded in rat-tail collagen, samples were shaken during all incubation steps, the primary antibody was incubated overnight at room temperature and the secondary antibody (1:400) was incubated for 4 h at room temperature, followed by four 15 min washes with PBS. Images of the samples were obtained with a Fluoview 1200 IX 83, hybrid confocal laser scanning / multiphoton microscope.

Intravital imaging

Skin flap surgery was performed on mice anaesthetized with Isoflurane before placing the tumor on a coverslip on top of an inverted hybrid confocal/multiphoton microscope, equipped with a multiphoton laser (MaiTai DeepSee) and a 30× immersion silicone objective (UPLSAPO30XSIR; NA: 1.05; Olympus). The selective EP4 agonist CAY10598 (Cayman; 100 μl of 1–10 μM) was injected intraperitoneally (250 μl of 10 μM), 3 h prior to imaging session. Presence of perfused blood vessels in chosen imaging area was confirmed prior to collecting each 4D stack. 4D stacks (14×5 μm) were collected at 3–5 min intervals, for up to 5 hours.

ImageJ was used for image processing and manual invadopodia counting. In our recently published work on breast carcinoma xenografts *in vivo*, we have demonstrated that invadopodia *in vivo* are highly dynamic protrusions whose assembly is limited to the perivascular niches (locations with major blood vessels, aligned collagen fibers and perivascular macrophages) (Gligorijevic et al., 2014). Invadopodia were the unique motility mode in such niches and can be identified by morphodynamic analysis. Briefly, morphodynamic analysis is done by first correcting timelapse recording for drift and breathing artefacts by StackReg (Thévenaz et al., 1998). Further, differential image is created by subtraction of frames taken at 0 and 3 (or 6) minutes, selecting for highly dynamic regions in the field of view. Finally, invadopodia can be localized and quantified using Particle Analysis by selecting for dynamic protrusions 2–20 μm^2 in size.

Statistical analysis

The effects of different chemical treatments on invasion, measured on two timepoints or only after 48 h, were analyzed using two-way ANOVA or one-way ANOVA, respectively. The effect of Mitomycin C on the invasion was analyzed using a Student's t-test. The effects of different chemical treatments and EP4 knock-down on the number of cells with mature invadopodia were analyzed using a generalized linear model. Invadopodia quantification from intravital imaging was analyzed with Mann-Whitney test.

Supplementary Material

Refer to Web version on PubMed Central for supplementary material.

Acknowledgments

We are grateful to Antoine Khalil and the Microscopic Imaging Center of the Radboud Institute for Molecular Life Sciences, Nijmegen for instrumental help, sharing protocols and resources. We also thank Yujin Chung from the Center for Computational Genetics and Genomics at Temple University for her help in statistical analysis. This work was supported by the Radboud Honours Academy to FT, EU grant NANOVISTA [grant number 2882630] to AC and United States National Institute of Health [NIH 5K99CA172360] to BG.

REFERENCES

An Q, Han C, Zhou Y, Li F, Li D, Zhang X, Yu Z, Duan Z, Kan Q. In vitro effects of mitomycin C on the proliferation of the non-small-cell lung cancer line A549. Int J Clin Exp Med. 2015; 8:20516–20523. [PubMed: 26884968]

Beaty BT, Condeelis J. Digging a little deeper: the stages of invadopodium formation and maturation. Eur. J. Cell Biol. 2014; 93:438–444. [PubMed: 25113547]

Bocca C, Ievolella M, Autelli R, Motta M, Mosso L, Torchio B, Bozzo F, Cannito S, Paternostro C, Colombatto S, Parola M, Miglietta A. Expression of Cox-2 in human breast cancer cells as a critical determinant of epithelial-to-mesenchymal transition and invasiveness. Expert Opin. Ther. Targets. 2014; 18:121–135. [PubMed: 24325753]

Boudreau N, Werb Z, Bissell MJ. Suppression of apoptosis by basement membrane requires three-dimensional tissue organization and withdrawal from the cell cycle. Proceedings of the National Academy of Sciences. 1996; 93:3509–3513.

Brocard E, Oizel K, Lalier L, Pecqueur C, Paris F, Vallette FM, Oliver L. Radiation-induced PGE2 sustains human glioma cells growth and survival through EGF signaling. Oncotarget. 2015; 6:6840–6849. [PubMed: 25749386]

Buchanan FG, Gorden DL, Matta P, Shi Q, Matrisian LM, DuBois RN. Role of beta-arrestin 1 in the metastatic progression of colorectal cancer. Proc. Natl. Acad. SciU.SA. 2006; 103:1492–1497.

Cortesio CL, Chan KT, Perrin BJ, Burton NO, Zhang S, Zhang Z-Y, Huttenlocher A. Calpain 2 and PTP1B function in a novel pathway with Src to regulate invadopodia dynamics and breast cancer cell invasion. The Journal of Cell Biology. 2008; 180:957–971. [PubMed: 18332219]

Cukierman E, Pankov R, Yamada KM. Cell interactions with three-dimensional matrices. Current opinion in cell biology. 2002; 14:633–639. [PubMed: 12231360]

Díaz B, Yuen A, Iizuka S, Higashiyama S, Courtneidge SA. Notch increases the shedding of HB-EGF by ADAM12 to potentiate invadopodia formation in hypoxia. The Journal of Cell Biology. 2013; 201:279–292. [PubMed: 23589494]

Du M, Shi F, Zhang H, Xia S, Zhang M, Ma J, Bai X, Zhang L, Wang Y, Cheng S, Yang Q, Leng J. Prostaglandin E2 promotes human cholangiocarcinoma cell proliferation, migration and invasion through the upregulation of β-catenin expression via EP3-4 receptor. Oncol. Rep. 2015; 34:715–726. [PubMed: 26058972]

Eckert MA, Lwin TM, Chang AT, Kim J, Danis E, Ohno-Machado L, Yang J. Twist1-induced invadopodia formation promotes tumor metastasis. Cancer Cell. 2011; 19:372–386. [PubMed: 21397860]

Fisher KE, Sacharidou A, Stratman AN, Mayo AM, Fisher SB, Mahan RD, Davis MJ, Davis GE. MT1-MMP- and Cdc42-dependent signaling co-regulate cell invasion and tunnel formation in 3D collagen matrices. Journal of Cell Science. 2009; 122:4558–4569. [PubMed: 19934222]

Friedl P, Sahai E, Weiss S, Yamada KM. New dimensions in cell migration. 2012; 13:743–747.

Fujino H, Regan JW. EP(4) prostanoid receptor coupling to a pertussis toxin-sensitive inhibitory G protein. Mol. Pharmacol. 2006; 69:5–10. [PubMed: 16204467]

Gligorijevic B, Bergman A, Condeelis J. Multiparametric classification links tumor microenvironments with tumor cell phenotype. PLoS Biol. 2014; 12:e1001995. [PubMed: 25386698]

Gligorijevic B, Wyckoff J, Yamaguchi H, Wang Y, Roussos ET, Condeelis J. N-WASP-mediated invadopodium formation is involved in intravasation and lung metastasis of mammary tumors. Journal of Cell Science. 2012; 125:724–734. [PubMed: 22389406]

Gould CM, Courtneidge SA. Regulation of invadopodia by the tumor microenvironment. Cell Adhesion & Migration. 2014

Kedziora KM, Leyton-Puig D, Argenzio E, Boumeester AJ, van Butselaar B, Yin T, Wu YI, van Leeuwen FN, Innocenti M, Jalink K, Moolenaar WH. Rapid remodeling of invadosomes by Gicoupled receptors: dissecting the role of Rho GTPases. J. Biol. Chem. 2016; 291 jbc.M115.695940–4333.

Kim JI, Lakshmikanthan V, Frilot N, Daaka Y. Prostaglandin E2 promotes lung cancer cell migration via EP4-betaArrestin1-c-Src signalsome. Molecular cancer research : MCR. 2010; 8:569–577. [PubMed: 20353998]

Konya V, Marsche G, Schuligoi R, Heinemann A. E-type prostanoid receptor 4 (EP4) in disease and therapy. Pharmacology & therapeutics. 2013; 138:485–502. [PubMed: 23523686]

Kundu N, Ma X, Kochel T, Goloubeva O, Staats P, Thompson K, Martin S, Reader J, Take Y, Collin P, Fulton A. Prostaglandin E receptor EP4 is a therapeutic target in breast cancer cells with stem-like properties. Breast Cancer Res. Treat. 2014; 143:19–31. [PubMed: 24281828]

Leong HS, Robertson AE, Stoletov K, Leith SJ, Chin CA, Chien AE, Hague MN, Ablack A, Carmine-Simmen K, McPherson VA, Postenka CO, Turley EA, Courtneidge SA, Chambers AF, Lewis JD. Invadopodia are required for cancer cell extravasation and are a therapeutic target for metastasis. Cell Rep. 2014; 8:1558–1570. [PubMed: 25176655]

Majumder M, Xin X, Liu L, Girish GV, Lala PK. Prostaglandin E2 receptor EP4 as the common target on cancer cells and macrophages to abolish angiogenesis, lymphangiogenesis, metastasis, and stem-like cell functions. Cancer Sci. 2014; 105:1142–1151. [PubMed: 24981602]

Martin TA, Ye L, Sanders AJ, Lane J, Jiang WG. Cancer Invasion and Metastasis: Molecular and Cellular Perspective. Landes Bioscience. 2000

Miglietta A, Toselli M, Ravarino N, Vencia W, Chiecchio A, Bozzo F, Motta M, Torchio B, Bocca C. COX-2 expression in human breast carcinomas: correlation with clinicopathological features and

prognostic molecular markers. Expert Opin. Ther. Targets. 2010; 14:655–664. [PubMed: 20536410]

Narumiya S, Sugimoto Y, Ushikubi F. Prostanoid receptors: structures, properties, and functions. Physiol. Rev. 1999; 79:1193–1226. [PubMed: 10508233]

Paquette B, Therriault H, Desmarais G, Wagner R, Royer R, Bujold R. Radiation-enhancement of MDA-MB-231 breast cancer cell invasion prevented by a cyclooxygenase-2 inhibitor. Br. J. Cancer. 2011; 105:534–541. [PubMed: 21792195]

Parida S, Pal I, Parekh A, Thakur B, Bharti R, Das S, Mandal M. GW627368X inhibits proliferation and induces apoptosis in cervical cancer by interfering with EP4/EGFR interactive signaling. Cell Death Dis. 2016; 7:e2154. [PubMed: 27010855]

Park B-W, Park S, Park HS, Koo JS, Yang WI, Lee JS, Hwang H, Kim SI, Lee KS. Cyclooxygenase-2 expression in proliferative Ki-67-positive breast cancers is associated with poor outcomes. Breast Cancer Res. Treat. 2012; 133:741–751. [PubMed: 22286316]

Patsialou A, Wyckoff J, Wang Y, Goswami S, Stanley ER, Condeelis JS. Invasion of human breast cancer cells in vivo requires both paracrine and autocrine loops involving the colony-stimulating factor-1 receptor. Cancer Res. 2009; 69:9498–9506. [PubMed: 19934330]

Pierce KL, Regan JW. Prostanoid receptor heterogeneity through alternative mRNA splicing. Life Sci. 1998; 62:1479–1483. [PubMed: 9585122]

Pignatelli J, Tumbarello DA, Schmidt RP, Turner CE. Hic-5 promotes invadopodia formation and invasion during TGF-β-induced epithelial-mesenchymal transition. The Journal of Cell Biology. 2012; 197:421–437. [PubMed: 22529104]

Rajadurai CV, Havrylov S, Zaoui K, Vaillancourt R, Stuible M, Naujokas M, Zuo D, Tremblay ML, Park M. Met receptor tyrosine kinase signals through a cortactin-Gab1 scaffold complex, to mediate invadopodia. Journal of Cell Science. 2012; 125:2940–2953. [PubMed: 22366451]

Regan JW. EP2 and EP4 prostanoid receptor signaling. Life Sci. 2003; 74:143–153. [PubMed: 14607241]

Sharma VP, Entenberg D, Condeelis J. High-resolution live-cell imaging and time-lapse microscopy of invadopodium dynamics and tracking analysis. Methods Mol. Biol. 2013; 1046:343–357. [PubMed: 23868599]

Sodek KL, Brown TJ, Ringuette MJ. Collagen I but not Matrigel matrices provide an MMP-dependent barrier to ovarian cancer cell penetration. BMC Cancer. 2008; 8:223. [PubMed: 18681958]

Stoletov K, Lewis JD. Invadopodia: a new therapeutic target to block cancer metastasis. Expert Rev Anticancer Ther. 2015; 15:733–735. [PubMed: 26098830]

Thévenaz P, Ruttimann UE, Unser M. A pyramid approach to subpixel registration based on intensity. IEEE Trans Image Process. 1998; 7:27–41. [PubMed: 18267377]

Tveteraas IH, Müller KM, Aasrum M, Ødegård J, Dajani O, Guren T, Sandnes D, Christoffersen T. Mechanisms involved in PGE2-induced transactivation of the epidermal growth factor receptor in MH1C1 hepatocarcinoma cells. J. Exp. Clin. Cancer Res. 2012; 31:72. [PubMed: 22967907]

Wolf K, Wu YI, Liu Y, Geiger J, Tam E, Overall C, Stack MS, Friedl P. Multi-step pericellular proteolysis controls the transition from individual to collective cancer cell invasion. Nat. Cell Biol. 2007; 9:893–904. [PubMed: 17618273]

Yamaguchi H, Wyckoff J, Condeelis J. Cell migration in tumors. Current opinion in cell biology. 2005; 17:559–564. [PubMed: 16098726]

Yokoyama U, Iwatsubo K, Umemura M, Fujita T, Ishikawa Y. The prostanoid EP4 receptor and its signaling pathway. Pharmacological reviews. 2013; 65:1010–1052. [PubMed: 23776144]

Zhang M, Zhang H, Cheng S, Zhang D, Xu Y, Bai X, Xia S, Zhang L, Ma J, Du M, Wang Y, Wang J, Chen M, Leng J. Prostaglandin E2 accelerates invasion by upregulating Snail in hepatocellular carcinoma cells. Tumour Biol. 2014; 35:7135–7145. [PubMed: 24760275]

Zhang X, Meng J, Wang Z-Y. A switch role of Src in the biphasic EGF signaling of ER-negative breast cancer cells. PLoS ONE. 2012; 7:e41613. [PubMed: 22927910]

Highlights

- Stimulation of EP4 promotes breast cancer cell invadopodia and invasion
- EP4-stimulated ECM degradation is EGFR dependent

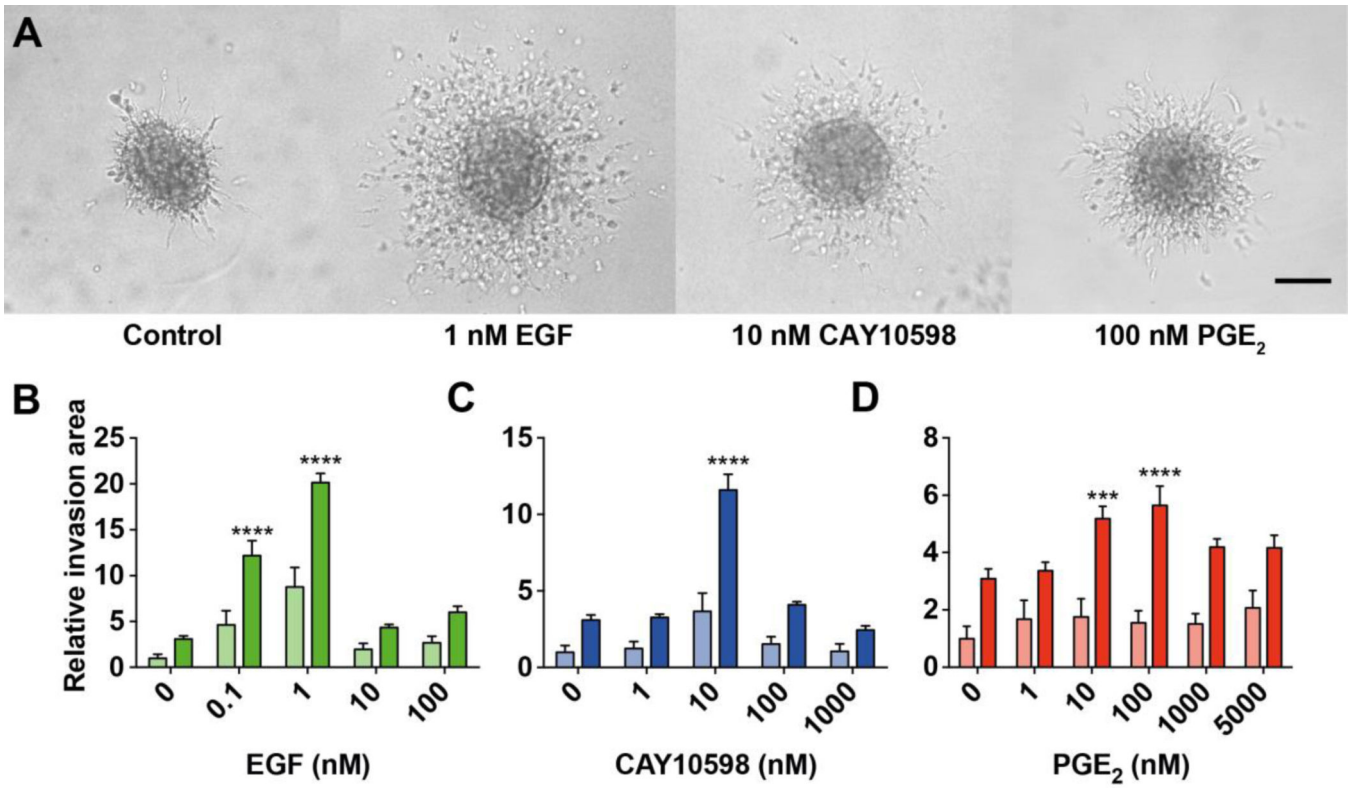

Figure 1. Dosage optimization of EGF, CAY10598 and PGE_2 in spheroid invasion assay

MDA-MB-231 spheroids were stimulated with EGF, CAY10598 (CAY) or PGE_2 to investigate involvement of EP4 and EGFR in invasive capability and to determine the optimal dosage. (**A**) Representative phase-contrast images of invasion of MDA-MB-231 spheroids (1,000 cells) embedded in rat tail collagen type I (4 mg/ml) control or stimulated with 1 nM EGF, 10 nM CAY10598 or 100 nM PGE_2 for 48 h. Scale bar= 100 μm (**B–D**) Light bars, 24 h treatment; dark bars, 48 h treatment. Values of all graphs present the mean + SEM of ten individual spheroids from one experiment. Two-way ANOVA was used for the statistical analysis. The asterisks show the significance of the difference compared to the 0 nM condition. *** P<0.001; **** P<0.0001.

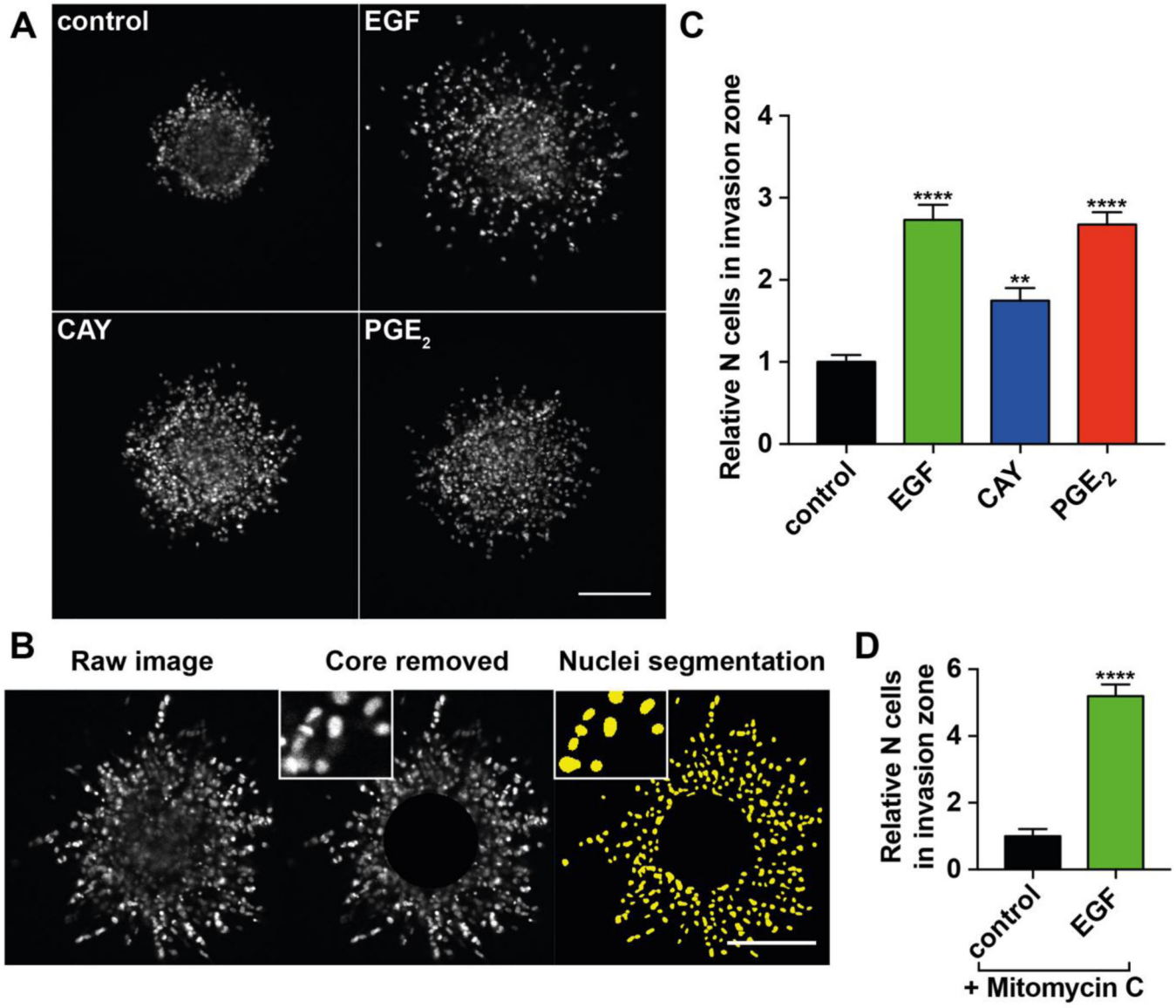

Figure 2. Spheroid invasion assay

(**A**) Representative images of MDA-MB-231 spheroids (1,000 cells) embedded in collagen I (5 mg/ml). Control spheroid treated with 1 nM DMSO and spheroids stimulated with 1 nM EGF, 10 nM CAY10598 (CAY) or 1 μM PGE_2 for 48 h were fixed and stained with DAPI. Scale bar= 200 μm. (**B**) Image processing workflow. The core of the spheroid was removed leaving only the cells in the invasion area for quantification. The nuclei were segmented and counted. (**C**) Quantification of cells in the invasion zone of spheroids shown in (A). Values present the mean + SEM of 15 – 25 spheroids per condition. One-way ANOVA was used for the statistical analysis. The asterisks show the significance of the difference compared to the DMSO control. ** P<0.01; **** P<0.0001. (**D**) Invasion assay in the presence of cell proliferation-inhibiting agent Mitomycin C (1 μg/μl). Values present the mean + SEM of 6 spheroids per condition. Students t-test was used for the statistical analysis. The asterisks show the significance of the difference compared to the DMSO control. **** P<0.0001.

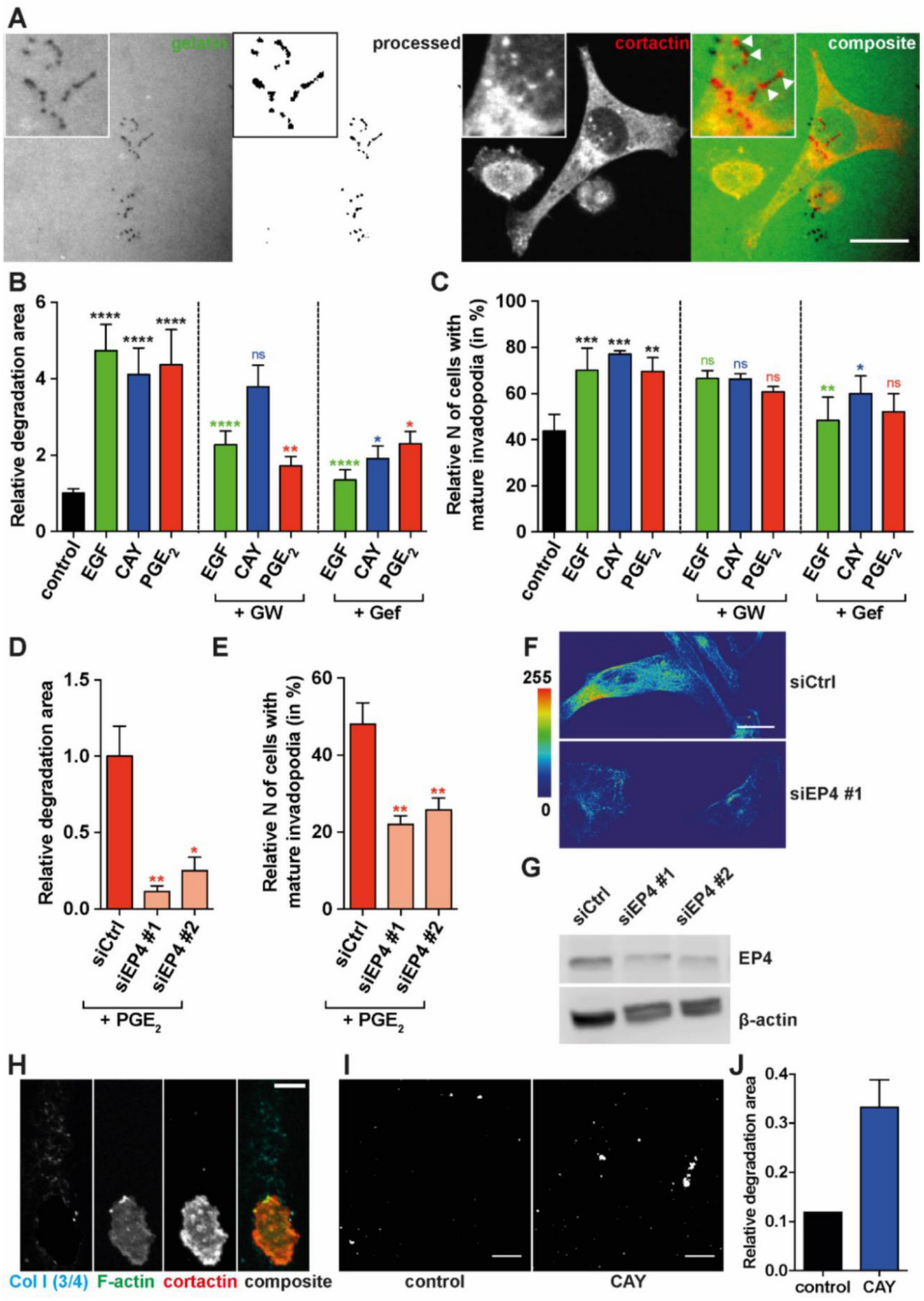

Figure 3. Degradation and invadopodia formation of MDA-MB-231 cells in 2D and 3D

Serum-starved MDA-MB-231 cells were plated on Oregon Green 488-labeled gelatin for 16 h; mature invadopodia were identified as co-localized punctae of gelatin degradation and cortactin. Examples are indicated by arrowheads. **(A)** Representative image of fluorescent gelatin, raw or processed, underneath the cells (1st and 2nd from left); MDA-MB-231 cell with invadopodia stained for cortactin on top of gelatin layer (3rd from left); composite of fluorescent gelatin and cortactin-stained cell (4th from left). Scale bar= 20 μm. Inserts zoom into mature invadopodia that degraded gelatin underneath; white arrows in composite insert

point to individual invadopodia. The area of degradation (**B**) and the number of cells with mature invadopodia (C) were determined. Values present the mean + SEM of ≥ 9 images from 3 biological repeats. The area of degradation (**D**) and the number of cells with mature invadopodia (E) was also determined in cells transfected with siCtrl, siEP4 #1/2, and treated with PGE_2. One-way ANOVA was used for the statistical analysis of area of degradation. Generalized linear regression model was used for the statistical analysis of number of cells with mature invadopodia. The color of the asterisks indicate the corresponding single treatment condition to which the statistical difference is displayed. * P<0.05; ** P<0.01; *** P<0.001; **** P<0.0001. (**F**) Representative pseudocolored images of MDA-MB-231 cells transfected with siCtrl or siEP4 #1 and stained for EP4 antibody. Pseudocolor look up table is shown on the left. (EP4 staining of siEP4 #1 and #2 showed similar results, not shown). (**G**) EP4 protein expression upon transfection with siCtrl, siEP4 #1/2 analyzed by Western Blot. Ratios of EP4/actin are 0.51 for siEP4 #1 and 0.52 siEP4 #2 compared to siCtrl. (**H**) Zoom into a cell in the invasion zone of MDA-MB-231 spheroids at 48 h and stained for collagen I (3/4), actin and cortactin. Scale bar= 10 μm. **(I)** Processed and thresholded images of collagen I (3/4) staining of spheroids- control and 10 nM CAY10598 (CAY) treatment. The degraded collagen is shown in white. Scale bar= 50 μm. **(J)** Quantification of degradation area of images from **(I)**.

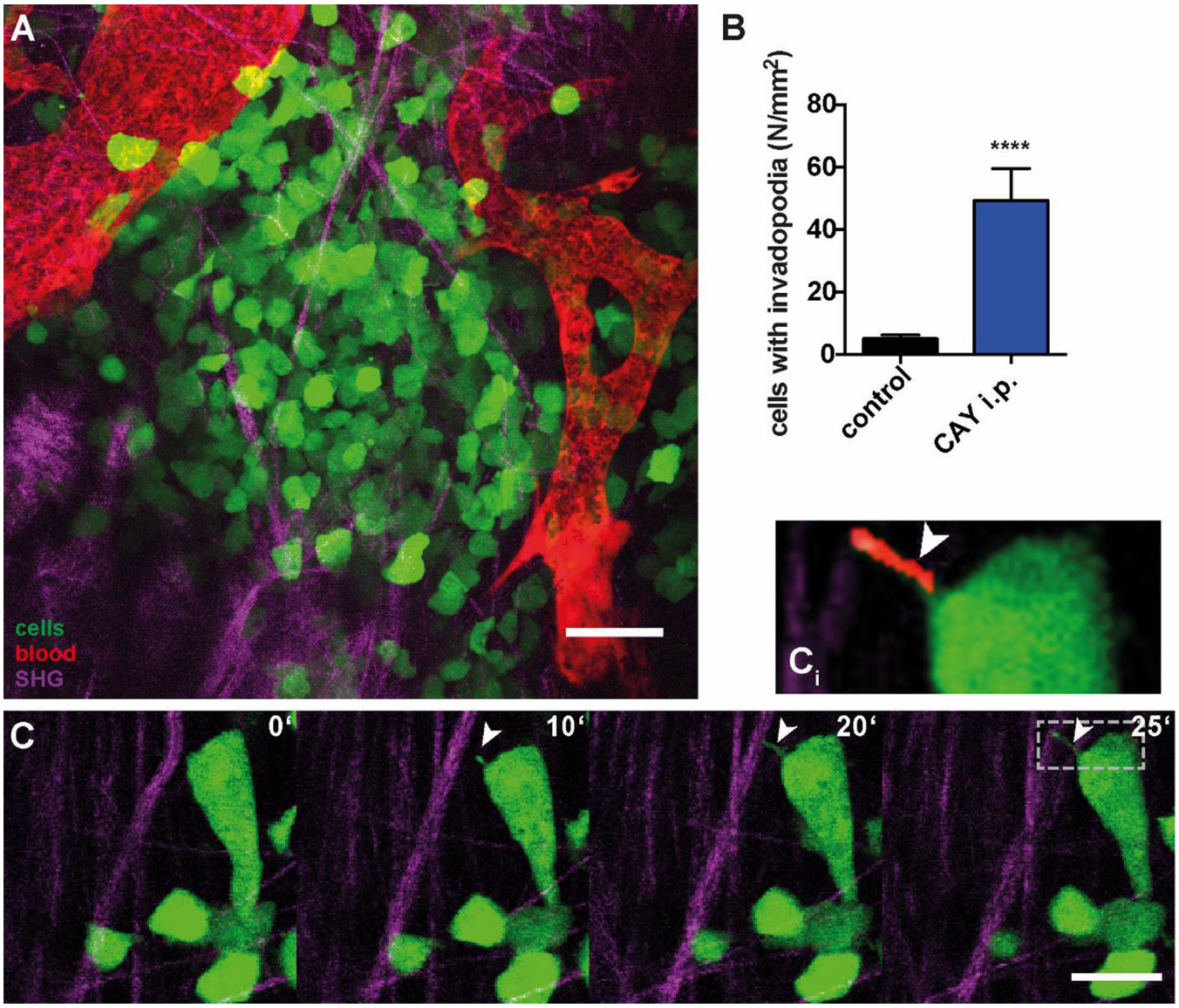

Figure 4. Systemic treatment with CAY10598 links EP4 stimulation with invadopodia formation in vivo

(**A**) Representative image (still of Video S1) of Dendra2-MDA-MB-231 xenograft in mammary fat pad of mice (green: Dendra2-MDA-MB-231 cells, magenta: SHG signal from collagen I fibers, red: blood vessels). (**B**) Quantification of invadopodia in 4D stacks of Dendra2-MDA-MB-231 xenograft control animals and 4 h after i.p. injection of CAY10598 (CAY). Values present the mean + SEM of ≥ 5 stacks from ≥ 2 animals. Mann-Whitney test was used for the statistical analysis; **** P<0.0001. (**C**) Stills from time-lapse (Video S2) of a cell extending invadopodium. (**C_i**) Insert zoom in to invadopodium; red denotes invadopodium detected by morphodynamic analysis. Scale bar= 20 μm.

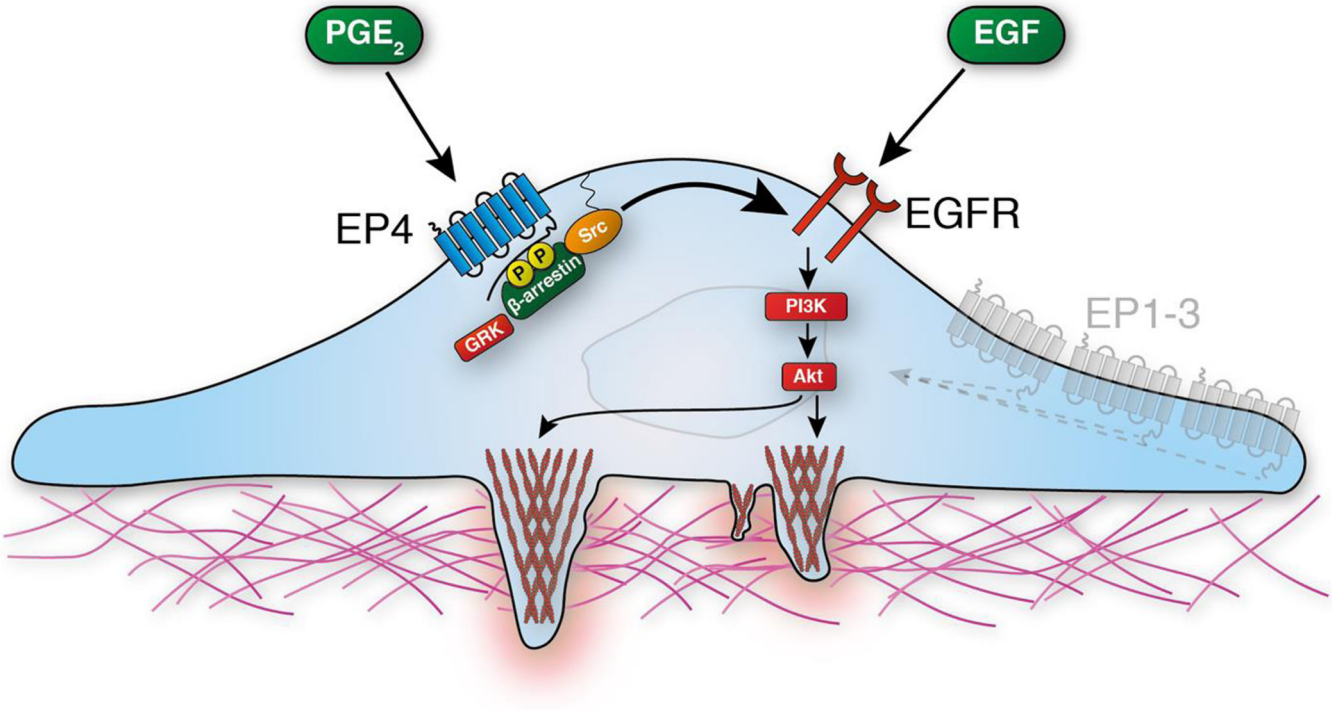

Figure 5. EP4 transactivates EGFR and thereby promotes the degradative capability of invadopodia

EP4 is activated by the endogenous pro-inflammatory lipid PGE_2. This leads to the phosphorylation of the activated EP4 by G protein-coupled receptor kinase (GRK) and allows recruitment and di-phosphorylation of β-arrestin and EGFR-dependent Src kinase phosphorylation. Further downstream phosphoinositide 3-kinase (PI3K) and the protein kinase B (Akt) stimulate invadopodia driven ECM degradation.